



Universiteit  
Leiden  
The Netherlands

## Stimulated raman adiabatic passage in optomechanics

Fedoseev, V.

### Citation

Fedoseev, V. (2022, July 7). *Stimulated raman adiabatic passage in optomechanics*. *Casimir PhD Series*. Retrieved from <https://hdl.handle.net/1887/3421649>

Version: Publisher's Version

License: [Licence agreement concerning inclusion of doctoral thesis in the Institutional Repository of the University of Leiden](#)

Downloaded from: <https://hdl.handle.net/1887/3421649>

**Note:** To cite this publication please use the final published version (if applicable).

## Introduction

In 1577 the Great Comet passed close to Earth. One of the best astronomical observers of the time, Tycho Brahe, noted that the comet's tail was pointing away from the Sun. Johannes Kepler, analyzing the data recorded by Brahe and observing another comet 30 years later, concluded that there must be radiation pressure pushing the comet's tail outwards from the Sun. In a letter to Galileo Galilei he hypothesized that one day this radiation pressure could be used for solar sails.

In 1872 James Clerk Maxwell put forward his theory of electromagnetism which gave a quantitative prediction of the radiation pressure. There were several attempts to measure the light pressure by illuminating a light mill in a vacuum chamber. The main difficulty was that the residual gas in the chamber complicated the interpretation of the measurements due to convection and radiometric forces. The first conclusive experimental observation was reported by Pyotr Lebedev in 1899 who managed to decrease the residual gas pressure to  $\sim 10^{-4}$  mbar by building a pump similar to the later introduced diffusion pumps.

It was shown by Vladimir Braginskii that there is a limit on the precision with which the position of an object can be continuously monitored [1]. This standard quantum limit (SQL) practically sets a lower bound on the sensitivity of optical interferometers, including gravitational wave detectors such as LIGO and VIRGO. Braginsky also proposed a way to beat the SQL by not measuring the position continuously, such measurements were termed quantum non-demolition (QND) measurements [2]. Nowadays these ideas are explored towards improving the sensitivity of the gravitational wave detectors.

Advances in the micro-electromechanical systems (MEMS) technology allowed to miniaturize optomechanical systems to the micro- and nano- scales. This allowed to reach GHz frequencies for optomechanically coupled oscillators. This is important as such mechanical oscillators are in a thermal state close to the ground state already at the dilution refrigerators temperatures, greatly facilitating experiments in the quantum regime [3, 4, 5].

Another step forward was made with the introduction of phononic crystals in optomechanical devices greatly enhancing the isolation of a mechanical mode from

its mechanical bath [6, 7].

Optomechanical devices are promising candidates to bridge disparate degrees of freedom like microwave and optical signals via a mechanical oscillator coupled to both fields [8]. This is essential in Quantum Information Science, for example for stationary (superconducting transmon) to flying (photon) qubit conversion.

Finally, optomechanical devices serve as ultra-sensitive probes of force, displacement, mass and acceleration [9] and provide a testbed for extensions of Quantum Mechanics [10].

Historically our group has a particular interest in studying massive superpositions and possible interplay of Quantum Mechanics and Gravity [11]. The idea behind it is that the gravitational self-energy might induce higher rates of decoherence than predicted by the standard quantum theory. These effects are predicted to become increasingly pronounced for larger test masses. This is one of the motivations for our group to work with relatively low frequency optomechanical devices naturally having higher effective masses. Therefore, lots of effort is put in the development of a low-vibration refrigeration capable of reaching the sub-mK regime.

## 1.1 Motivation and outlook

The goal of the work presented in this thesis is to build an optomechanical system based on the membrane-in-the-middle configuration operating in the quantum regime and to develop a method for a quantum state transfer between two mechanical oscillators coupled to a common optical mode.

Mechanical modes have long coherence times and can be used in quantum information as quantum memory. Therefore, a state transfer between mechanical modes may be an important tool for Quantum Information Science. It appears that the process of a state transfer can be stopped in the middle of the process and the mechanical modes become entangled [12, 13]. This brings a possibility to realize entanglement between massive oscillators which is an achievement on itself. Studies of the evolution of entangled oscillators with increasing masses may probe the parameter space where some theories predict new physics beyond predictions based on the model of environment induced decoherence in standard quantum mechanics. [11].

Several methods of a state transfer in optomechanics were demonstrated [14, 12, 15]. The demonstrated state transfer efficiency in the topological energy transfer [14, 15] was about 0.1 which is quite low. The two tone swapping method [12] requires precise control over the experimental parameters: the difference in the frequencies of the driving light tones should be equal to the difference in the mechanical frequencies of the modes adjusted by the optical spring effect within the mechanical linewidth. It is hard to realize experimentally for very high quality mechanical modes.

Stimulated Raman Adiabatic Passage (STIRAP) is a technique for a population transfer which is both robust to uncertainties in the experimental parameters and can achieve high state transfer efficiencies [16, 13]. This is a well-established technique demonstrated in many physical systems but not in optomechanics. The work shown in this thesis was to analyze the feasibility and requirements of STIRAP in op-

tomechanics as well as towards experimental realization of STIRAP of a non-classical state between two vibrational modes in the MHz range.

In section 2 of this chapter we discuss the main optomechanical concepts and effects encountered throughout this thesis. Section 3 introduces the system we are working with - a membrane inside a high finesse optical cavity.

The work presented in this thesis started with building a membrane-in-the-middle setup using a commercial SiN membrane. Chapter 2 presents a strong squeezing of a thermal mechanical state achieved in this system by parametric modulation of the optical spring effect.

Next, we introduced a phononic crystal membrane into this cavity fabricated in our group in UC Santa Barbara. These membranes possess 1-2 orders of magnitude higher mechanical quality factors for vibrational modes localized in the defect of the phononic crystal. High mechanical quality factors and the phononic crystal bandgap allowed the realization of a high efficiency state transfer between two vibrational modes of the same membrane through the optical mode using STIRAP. Such a state transfer of a classical state at room temperature is described in Chapter 3.

Chapter 4 discusses a possibility to realize STIRAP of single-phonon Fock state between two in-gap membrane modes. We show that a state transfer with fidelity of 0.6 is feasible assuming system parameters achieved in state-of-the-art devices at 1 K with single photon detection by superconducting nanowire single photon detectors. We also discuss a possibility to entangle two membrane modes and detect such an entanglement using a modified version of STIRAP.

Next, the design and fabrication of a novel cryogenic compatible optical cavity is presented. In Chapter 5 we characterize this cavity and demonstrate optical coupling to a single mode optical fiber  $> 0.9$  at cryogenic temperatures.

In Chapter 6 we discuss a setup for quantum optomechanical experiments based on detection of Stokes and anti-Stokes photons. For example, it would be possible to realize STIRAP of a single-phonon state described in Chapter 4 using this setup. Such a setup is under construction in our lab.

In Chapter 7 we investigate the feasibility of measuring the average phonon occupation of a thermal state close to the quantum ground state in our system using a balanced heterodyne detection scheme. We found that it is not possible to do such a measurement without sending relatively strong probe light fields which most likely will heat the membrane. To do a measurement where the heating by the intracavity light fields of a probe light is weaker than the heating by the cooling light, single photon detection described in Chapter 6 is required.

The work presented in this thesis is summarized in Chapter 8 in connection to previous and future work in our lab.

## 1.2 Basic optomechanics

A generic optomechanical system based on a Fabry-Perot resonator is depicted in Fig. 1.1. The Fabry-Perot resonator (which will be further referred to as the optical cavity) consists of two high reflectivity mirrors where one of the mirrors is fixed while the other mirror is attached to a spring. The movable mirror on a spring system has a resonance frequency  $\Omega$ .

Let's find the evolution of the intracavity light fields. Light with frequency  $\omega_L$  and electric field amplitude  $E_{\text{in}}$  is sent to the cavity. Light entering the cavity will be reflected inside the cavity many times. Interference of these reflections will result in an intracavity light field amplitude  $E$ . In the steady state situation:

$$E = E_{\text{in}}t + E_{\text{in}}tr^2e^{i\phi} + E_{\text{in}}t(r^2e^{i\phi})^2 + \dots, \quad (1.1)$$

where  $t$  and  $r$  are amplitude transmissivity and reflectivity of each mirror (mirrors are ideal and identical,  $r^2 + t^2 = 1$ ) and  $\phi$  is accumulated phase in one round trip  $\phi = 2\pi/\lambda \times 2L = \frac{\omega_L}{c} \times 2L$  with  $\lambda$  the wavelength of light,  $L$  the cavity length and  $c$  the speed of light. For this derivation we consider flat parallel mirrors for simplicity with plane waves  $E_{\text{in}}$ . Performing the summation in Eq. 1.1 we get

$$E = \frac{E_{\text{in}}t}{1 - r^2e^{i\phi}}. \quad (1.2)$$

The incoming light fields are on resonance with the cavity when  $e^{i\phi} = 1$  corresponding to the frequency  $\omega_{\text{cav}}$  such that  $e^{i\frac{2L}{c}\omega_{\text{cav}}} = 1$  and the intracavity light fields amplitude  $E = E_{\text{in}}/t$ . Let's introduce the detuning  $\Delta$  from the cavity resonance  $\Delta = \omega_L - \omega_{\text{cav}}$ . For the detuning values much smaller than the frequency between the two adjacent resonances which is equivalent to  $|\phi| \ll 1$

$$e^{i\phi} = e^{i\frac{2L}{c}\omega_L} = e^{i\frac{2L}{c}\omega_L} e^{-i\frac{2L}{c}\omega_{\text{cav}}} = e^{i\frac{2L}{c}\Delta} \approx 1 + i\Delta \frac{2L}{c}. \quad (1.3)$$

Equation 1.2 can be written as

$$E_{\text{in}}t = E(1 - r^2e^{i\phi}) \approx E(1 - (1 - t^2)(1 + i\Delta \frac{2L}{c})) \approx Et^2(1 - i\Delta \frac{2L}{ct^2}). \quad (1.4)$$

We see that the intracavity light amplitude is a function of the distance between the mirrors. Therefore, the mechanical motion of the movable mirror affects the intracavity light fields. Further we will see that there is also a reverse effect where the intracavity light affects the motion of the mirror - hence the name optomechanics.



Figure 1.1: Basic optomechanical system.

Let's consider a situation where the incoming light fields are abruptly switched off. The intracavity light will decay. To find the decay rate let's consider photons inside the cavity. The probability of a photon to leave the cavity via one of the mirrors is  $t^2$ , each photon impinges on a mirror every  $L/c$  seconds, thus the energy decay rate  $\kappa = t^2/(L/c)$ . The intracavity electric field will decay as

$$\dot{E} = -\frac{\kappa}{2}E. \quad (1.5)$$

The 2 in the denominator comes from the fact that energy ( $\propto E^2$ ) decays with the rate  $\kappa$ , electric field  $E$  decays with the rate  $\kappa/2$ .

Now we introduce the frame rotating at  $\omega_{\text{cav}}$  and find the electric field in this frame  $E_{\text{cav}}$ . Recalling that  $E$  is the field amplitude, the intracavity field changes with time as

$$E(t) = Ee^{i\omega_L t} = E_{\text{cav}}e^{i\omega_{\text{cav}} t}, \quad (1.6)$$

therefore

$$E = E_{\text{cav}}e^{i(\omega_{\text{cav}} - \omega_L)t} = E_{\text{cav}}e^{-i\Delta t}, \quad (1.7)$$

where  $\Delta = \omega_L - \omega_{\text{cav}}$  is the light fields detuning. Substituting  $E$  from Eq. 1.7 into Eq. 1.5 we get

$$\dot{E}_{\text{cav}} = -\frac{\kappa}{2}E_{\text{cav}} + i\Delta E_{\text{cav}}. \quad (1.8)$$

Returning to the case of the steady state situation Eq. 1.4 can be written as

$$0 = -\frac{\kappa}{2}E_{\text{cav}} + i\Delta E_{\text{cav}} + \sqrt{\kappa_{\text{ext}}}\sqrt{\frac{c}{2L}}E_{\text{in}}, \quad (1.9)$$

where we introduced the coupling rate of the incoming light fields  $\kappa_{\text{ext}} = \kappa/2$ . Generalizing Eq. 1.8 and 1.9 for a non-steady state we get

$$\dot{E}_{\text{cav}} = -\frac{\kappa}{2}E_{\text{cav}} + i\Delta E_{\text{cav}} + \sqrt{\kappa_{\text{ext}}}\sqrt{\frac{c}{2L}}E_{\text{in}}, \quad (1.10)$$

To find the quantum analog of Eq. 1.10 we need the expressions for the incoming light intensity

$$I_{\text{in}} = \frac{1}{2}c\epsilon_0|E_{\text{in}}|^2 = \hbar\omega_L\langle\hat{a}_{\text{in}}^\dagger\hat{a}_{\text{in}}\rangle \quad (1.11)$$

and the energy of the intracavity light fields

$$W = I_{\text{cav}}\frac{2L}{c} = \frac{1}{2}c\epsilon_0|E_{\text{cav}}|^2 \times \frac{2L}{c} = \hbar\omega_L\langle\hat{a}^\dagger\hat{a}\rangle, \quad (1.12)$$

where  $\epsilon_0$  is the vacuum dielectric permittivity,  $a_{\text{in}}$  is the quantum field corresponding to the incoming light fields,  $I_{\text{cav}}$  is the intracavity light intensity corresponding to the running wave with amplitude  $E_{\text{cav}}$  and  $\hat{a}$  is the intracavity quantum field. Using these expressions we get

$$\dot{\hat{a}} = -\frac{\kappa}{2}\hat{a} + i\Delta\hat{a} + \sqrt{\kappa_{\text{ext}}}\hat{a}_{\text{in}}. \quad (1.13)$$

Equation 1.13 is identical to the general one describing the evolution of the intracavity light fields [9] in the absence of any incoming noise  $\hat{f}_{\text{in}}$ . We showed here an intuition behind this equation rather than its derivation.

Next, we consider how the intracavity light affects the motion of an optomechanically coupled oscillator. For the simple case shown in Fig. 1.1 the equation of motion of the movable mirror is

$$\ddot{x} + \Gamma_m \dot{x} + \Omega^2 x = \frac{F}{m}, \quad (1.14)$$

where  $x$  is the shift of the mirror along the optical axis,  $\Gamma_m = \Omega/Q$  is the damping rate and  $Q$  is the mechanical quality factor,  $m$  is the mirror mass and  $F$  is the radiation pressure force due to the intracavity light fields  $\hat{a}$ . Each photon transfers a momentum  $2\hbar\omega_L/c$  each  $2L/c$  seconds, resulting in the overall force

$$F = (2\hbar\omega_L/c)/(2L/c)\langle\hat{a}^\dagger\hat{a}\rangle = \hbar\frac{\omega_L}{L}\langle\hat{a}^\dagger\hat{a}\rangle. \quad (1.15)$$

Generally, the force is

$$F = \hbar G \langle\hat{a}^\dagger\hat{a}\rangle, \quad (1.16)$$

where we introduced optomechanical coupling  $G = -\partial\omega_{\text{cav}}/\partial x$ , in our case  $G = \frac{\omega_L}{L}$ .

In the case of a high- $Q$  mechanical oscillator Eq. 1.14 can be simplified to a first order differential equation because the amplitude of oscillations cannot change fast [9]. Let's use this property:

$$x = Ae^{-i\Omega t}, \dot{x} = \dot{A}e^{-i\Omega t} - i\Omega Ae^{-i\Omega t}, \ddot{x} = -2i\Omega\dot{A}e^{-i\Omega t} - \Omega^2 Ae^{-i\Omega t}, \quad (1.17)$$

where we neglected the term containing  $\ddot{A}$ . Using Eq. 1.17 and 1.14 we get

$$-2i\Omega\dot{A}e^{-i\Omega t} - i\Omega\Gamma_m Ae^{-i\Omega t} = \frac{F}{m}, \quad (1.18)$$

where we neglected the term containing  $\dot{A}$  ( $\Gamma$  and  $\dot{A}$  are small). Going back to the non-rotating frame  $x = Ae^{-i\Omega t}$  we get

$$\dot{x} = \left(-\frac{\Gamma_m}{2} - i\Omega\right)x + i\frac{F}{2m\Omega}. \quad (1.19)$$

The quantum version of this equation is [9]

$$\dot{\hat{b}} = \left(-\frac{\Gamma_m}{2} - i\Omega\right)\hat{b} + i\frac{\hat{F}}{2m\Omega x_{\text{zpf}}}, \quad (1.20)$$

where  $\hat{x} = x_{\text{zpf}}(\hat{b} + \hat{b}^\dagger)$  and  $x_{\text{zpf}} = \sqrt{\langle 0|\hat{x}^2|0\rangle} = \sqrt{\frac{\hbar}{2m\Omega}}$  is the zero point fluctuation amplitude,  $|0\rangle$  is the mechanical vacuum state. Using Eq. 1.16 we get

$$\dot{\hat{b}} = \left(-\frac{\Gamma_m}{2} - i\Omega\right)\hat{b} + ig_0\hat{a}^\dagger\hat{a}, \quad (1.21)$$

where  $g_0 = Gx_{\text{zpf}}$  is the single photon optomechanical coupling rate.

Equation 1.21 together with Eq. 1.13 written in the form

$$\dot{\hat{a}} = -\frac{\kappa}{2}\hat{a} + i(\Delta_0 + g_0(\hat{b} + \hat{b}^\dagger))\hat{a} + \sqrt{\kappa_{\text{ext}}}\hat{a}_{\text{in}} \quad (1.22)$$

are the basic optomechanical equations governing the dynamics of the interaction of light fields and an optomechanically coupled oscillator. The classical version of these two coupled differential equations is used in Chapter 3.

Next, we expand the detuning  $\Delta$  from Eq. 1.13 into  $\Delta = \Delta_0 + \hat{x}\partial\Delta/\partial x = \Delta_0 + G\hat{x}$  and  $\hat{x} = x_{\text{zpf}}(\hat{b} + \hat{b}^\dagger)$ , where  $\Delta_0$  is the unperturbed laser detuning.

The energy of an optomechanical system consists of the energy of the photons  $\hbar\omega_L\langle\hat{a}^\dagger\hat{a}\rangle$ , energy of the phonons  $\hbar\Omega\langle\hat{b}^\dagger\hat{b}\rangle$ , and their interaction energy. The interaction part is the potential energy of the oscillator  $-\langle\hat{F}\hat{x}\rangle = -\hbar g_0\langle\hat{a}^\dagger\hat{a}(\hat{b} + \hat{b}^\dagger)\rangle$ . Now we can write the full Hamiltonian of an optomechanical system

$$\hat{H} = \hbar\omega_L\hat{a}^\dagger\hat{a} + \hbar\Omega\hat{b}^\dagger\hat{b} - \hbar g_0\hat{a}^\dagger\hat{a}(\hat{b} + \hat{b}^\dagger). \quad (1.23)$$

In Chapter 4 we use Eq. 1.23 to simulate the dynamics of an optomechanical system via the Linblad formalism requiring a Hamiltonian.

Next, we consider an oscillator in thermal equilibrium with a thermal bath at temperature  $T$ . The oscillator has a mechanical susceptibility defined through  $x(\omega) = \chi(\omega)F(\omega)$

$$\chi_m(\omega) = \frac{1}{2m\Omega(\Omega - \omega - i\Gamma_m/2)}, \quad (1.24)$$

where  $x(\omega)$  is the Fourier transform of the oscillator position  $x$  and  $F(\omega)$  is the Fourier transform of the external force applied to the oscillator. The power spectral density (PSD) of the oscillator relates to the mean square of  $x$  via

$$\frac{1}{2\pi} \int_{-\infty}^{\infty} S_{xx}(\omega) d\omega = \langle x^2 \rangle. \quad (1.25)$$

The fluctuation dissipation theorem relates  $S_{xx}(\omega)$  to the mechanical response  $\chi_m(\omega)$  in thermal equilibrium [9]:

$$S_{xx}(\omega) = \frac{2kT}{\omega} \text{Im}\chi_m(\omega) = \frac{kT}{2m\Omega^2} \frac{\Gamma_m}{(\omega - \Omega)^2 + \Gamma_m^2/4}. \quad (1.26)$$

These relationships allow us to calculate the PSD of the force exerted by the bath on the oscillator:

$$S_{FF}(\omega) = \frac{S_{xx}(\omega)}{|\chi_m(\omega)|^2} = 2kTm\Gamma_m. \quad (1.27)$$

Next, we consider the case when a constant intensity light fields with detuning  $\Delta$  is sent to the cavity with an optomechanically coupled oscillator. The dynamics of the oscillator can be found by solving Eq. 1.21 and 1.22. The radiation pressure backaction alters the mechanical susceptibility to

$$\chi(\omega) = \frac{1}{2m\Omega((\Omega + \delta\Omega_{\text{opt}}) - \omega - i(\Gamma_m + \Gamma_{\text{opt}})/2)}, \quad (1.28)$$



with

$$\delta\Omega_{\text{opt}} = g_0^2 n_{\text{cav}} \left( \frac{\Delta - \Omega}{(\Delta - \Omega)^2 + \kappa^2/4} + \frac{\Delta + \Omega}{(\Delta + \Omega)^2 + \kappa^2/4} \right) \quad (1.29)$$

$$\Gamma_{\text{opt}} = g_0^2 n_{\text{cav}} \left( \frac{\kappa}{(\Delta + \Omega)^2 + \kappa^2/4} - \frac{\kappa}{(\Delta - \Omega)^2 + \kappa^2/4} \right) \quad (1.30)$$

under the assumption of small intracavity photon number  $n_{\text{cav}}$  resulting in  $\Gamma_{\text{opt}} \ll \kappa$ . Now the oscillator is not in thermal equilibrium with the bath. Let's find its mean square motion  $\langle x^2 \rangle$ . Though the mechanical susceptibility has changed to Eq. 1.28 the oscillator is still driven by the thermal force given by Eq. 1.27:

$$S_{xx}(\omega) = S_{FF}(\omega) |\chi(\omega)|^2 = \frac{kT}{2m\Omega^2} \frac{\Gamma_m}{(\omega - \Omega)^2 + (\Gamma_m + \Gamma_{\text{opt}})^2/4}. \quad (1.31)$$

Comparing this result to Eq. 1.26 we find

$$\langle x^2 \rangle = \frac{1}{2\pi} \int_{-\infty}^{\infty} S_{xx}(\omega) d\omega = \frac{\Gamma_m}{\Gamma_m + \Gamma_{\text{opt}}} \langle x^2 \rangle|_{n_{\text{cav}}=0}. \quad (1.32)$$

Now we can define the effective temperature  $T_{\text{eff}}$  satisfying the fluctuation-dissipation theorem:

$$T_{\text{eff}} = \frac{\Gamma_m}{\Gamma_m + \Gamma_{\text{opt}}} T. \quad (1.33)$$

Finding  $T_{\text{eff}}$  for an oscillator in the quantum regime requires consideration of the rates of the probabilities of the oscillator transitioning from the state with  $n$  phonons to the state of  $n + 1$  phonons [17]

$$\gamma_{n \rightarrow n+1} = \frac{x_{\text{zpf}}^2}{\hbar^2} (n+1) S_{FF}(-\Omega) \quad (1.34)$$

and the rates of the probabilities of the oscillator transitioning from the state with  $n$  phonons to the state of  $n - 1$  phonons

$$\gamma_{n \rightarrow n-1} = \frac{x_{\text{zpf}}^2}{\hbar^2} n S_{FF, \text{total}}(\Omega). \quad (1.35)$$

In this case a bare mechanical oscillator is considered with  $S_{FF, \text{total}}$  being the total PSD due to the radiation pressure forces and the forces from the mechanical bath. The final phonon occupation  $\bar{n}_f$  is obtained by finding a steady state when the probabilities of the oscillator to occupy a state  $n$  are not changing in time. This gives [17]:

$$\bar{n}_f = \frac{\gamma_{0 \rightarrow 1}}{\gamma_{1 \rightarrow 0} - \gamma_{0 \rightarrow 1}}. \quad (1.36)$$

Considering the same probabilities it can be shown that the state  $\bar{n}_f$  is approached with the rate  $\Gamma = \gamma_{1 \rightarrow 0} - \gamma_{0 \rightarrow 1}$ , therefore this rate is the energy decay rate as defined above.

If the oscillator is coupled to the mechanical bath only, it has the phonon population  $\bar{n}_{f,m} = n_{\text{th}} = \frac{kT}{\hbar\Omega}$  for  $kT \gg \hbar\Omega$  and has the energy decay  $\gamma_{1 \rightarrow 0} - \gamma_{0 \rightarrow 1} = \Gamma_m$ .

If the oscillator is coupled to the optical bath only, the PSD of the forces acting on it is [17]:

$$S_{FF,\text{opt}}(\omega) = \frac{\hbar^2}{x_{\text{zpm}}^2} g_0^2 n_{\text{cav}} |\chi_{\text{opt}}(\omega)|^2, \quad (1.37)$$

where  $\chi_{\text{opt}}(\omega) = \frac{\sqrt{\kappa}}{\kappa/2 + i(\Delta - \omega)}$  is the optical susceptibility of the cavity. Now we can find the steady state phonon occupation of an oscillator coupled to the optical bath only using Eq. 1.37 and 1.36:

$$\bar{n}_{f,\text{opt}} = \frac{|\chi_{\text{opt}}(-\Omega)|^2}{|\chi_{\text{opt}}(\Omega)|^2 - |\chi_{\text{opt}}(-\Omega)|^2}. \quad (1.38)$$

The energy decay of the oscillator in this case is

$$\Gamma_{\text{opt}} = g_0^2 n_{\text{cav}} (|\chi_{\text{opt}}(\Omega)|^2 - |\chi_{\text{opt}}(-\Omega)|^2), \quad (1.39)$$

which coincides with Eq. 1.30.

Finally, we can find the steady state when the oscillator is coupled to the optical and mechanical baths simultaneously. As the optical and thermal forces are independent the total PSD of the force is the sum of the mechanical and optical components:

$$S_{FF,\text{total}}(\omega) = S_{FF,m}(\omega) + S_{FF,\text{opt}}(\omega). \quad (1.40)$$

Therefore,

$$\bar{n}_f = \frac{\gamma_{0 \rightarrow 1,m} + \gamma_{0 \rightarrow 1,\text{opt}}}{(\gamma_{1 \rightarrow 0,m} + \gamma_{1 \rightarrow 0,\text{opt}}) - (\gamma_{0 \rightarrow 1,m} + \gamma_{0 \rightarrow 1,\text{opt}})} = \quad (1.41)$$

$$= \frac{\gamma_{0 \rightarrow 1,m} + \gamma_{0 \rightarrow 1,\text{opt}}}{\Gamma_m + \Gamma_{\text{opt}}}. \quad (1.42)$$

Using Eq. 1.36 we are getting  $\gamma_{0 \rightarrow 1,j} = \Gamma_j \bar{n}_{f,j}$  and finally

$$\bar{n}_f = \frac{\Gamma_m n_{\text{th}} + \Gamma_{\text{opt}} n_{\text{min}}}{\Gamma_m + \Gamma_{\text{opt}}}, \quad (1.43)$$

where  $n_{\text{min}} = \bar{n}_{f,\text{opt}}$  from Eq. 1.38.

## 1.3 Membrane-in-the-middle

In this section we discuss an optical cavity with a transparent dielectric membrane in the middle. The reflectivity of the membrane is given by [18]

$$r_d = \frac{(n^2 - 1) \sin(\frac{2\pi}{\lambda} n L_d)}{2i n \cos(\frac{2\pi}{\lambda} n L_d) + (n^2 + 1) \sin(\frac{2\pi}{\lambda} n L_d)}, \quad (1.44)$$

where  $n$  is the refractive index of the membrane and  $L_d$  is the thickness of the membrane. In this thesis we are discussing two SiN membranes with  $n \approx 2$ , one with thickness 50 nm in Chapter 2, all the other chapters are based on a membrane with

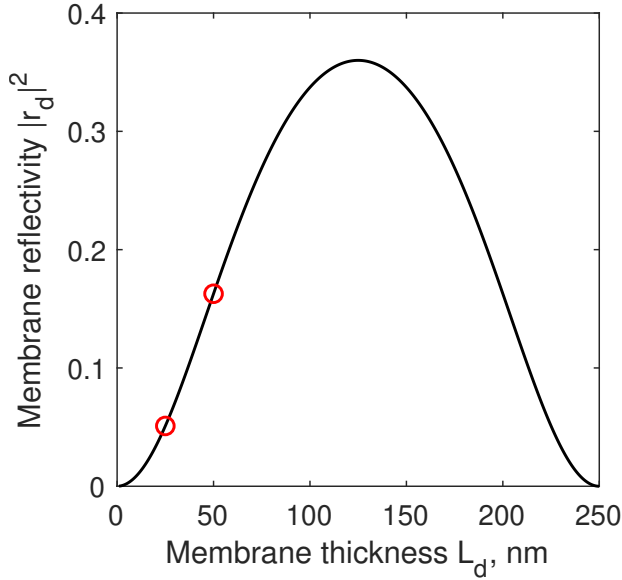


**Figure 1.2:** Theoretical reflectivity of a SiN membrane as a function of thickness. The red circles represent theoretical values for the two membranes used in this thesis with  $L_d = 25$  nm and  $L_d = 50$  nm.

thickness 25 nm. Theoretical intensity reflectivity  $|r_d|^2$  is plotted in Fig. 1.2 as a function of the membrane thickness. Membrane acts as a Fabry-Perot resonator which gives rise to the shape of this curve.

Solving the boundary condition equations for the electromagnetic wave in the cavity with a membrane results in the following equation under the assumption of  $\text{Im}(n) = 0$  and cavity mirror reflectivities  $r_m \rightarrow 1$  [18]:

$$\omega_{\text{cav}}(x) = \frac{c}{L} \arccos(|r_d| \cos \frac{2\pi}{\lambda} x), \quad (1.45)$$

where  $c$  is the speed of light. Here  $x$  is a membrane shift from the cavity center on the wavelength scale. The theoretical cavity-with-membrane resonant frequency  $\omega_{\text{cav}}$  is plotted in Fig. 1.3 for various membrane reflectivities.

The membrane-in-the-middle system differs from the system with one fixed mirror and one movable mirror depicted in Fig. 1.1 and it's not straightforward to see how the optomechanical coupling arises in the membrane-in-the-middle system. Generally, the intensities of light at the left membrane boundary and at the right one are different. This is true for all membrane positions except for the nodes and antinodes. The difference in the intensities gives rise to non-zero net radiation pressure and thus to optomechanical coupling. Mathematically the dependence of the cavity resonance frequency on the membrane position  $\omega_{\text{cav}}(x)$  as seen in Fig. 1.3 gives rise to the optomechanical coupling.

Another important difference with the system with a moving mirror is that the difference of the consecutive cavity resonance frequencies is a function of the mem-

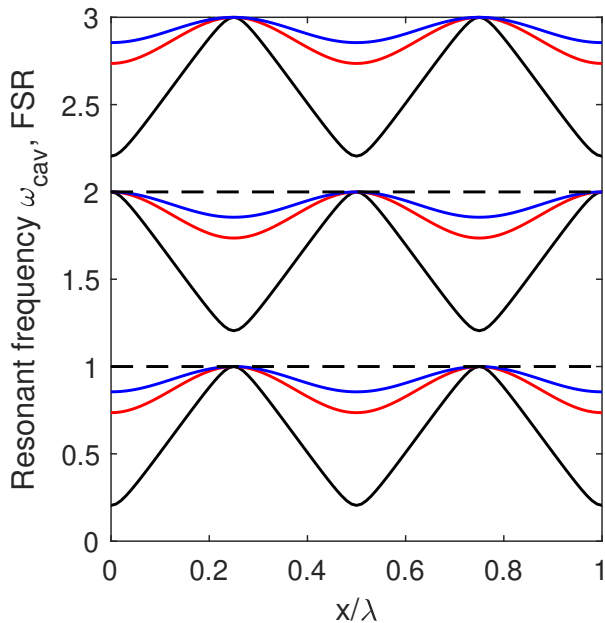


**Figure 1.3:** Resonant frequency of a cavity with a SiN membrane in the middle as a function of the membrane position  $x$  for different membrane reflectivities. The dashed line corresponds to  $|r_d|^2 = 0$  (empty cavity), the blue line corresponds to membrane thickness  $L_d = 25$  nm and  $|r_d|^2 = 0.05$ , red to  $L_d = 50$  nm and  $|r_d|^2 = 0.16$ , black to  $|r_d|^2 = 0.9$ .

brane position while the odd or even cavity resonances have constant frequency difference which we further will call  $2\text{FSR}$ .

